Ab initio study of OH-functionalized single-wall carbon nanotubes

H. Pan, Y. P. Feng,* and J. Y. Lin
Department of Physics, National University of Singapore, 2 Science Drive 3, 117542 Singapore
(Received 15 January 2004; revised manuscript received 1 June 2004; published 21 December 2004)

The effects of the OH group on the electronic and optical properties of single-wall carbon nanotubes were investigated using first principles electronic structure calculations. Our results confirm band-gap reduction of semiconductor carbon nanotubes up on addition of the OH group. An additional energy level emerges near the Fermi level, which is due to coupling between one *p* orbital of the oxygen with the big π bond of the nanotube. Analysis of loss function showed that the plasmon excitation shifts to lower frequency.

DOI: 10.1103/PhysRevB.70.245425 PACS number(s): 61.48.+c, 68.43.−h, 73.22.−f, 71.15.Mb

Functionalization of single-wall carbon nanotubes (SWCNTs) through chemical binding of atoms, molecules, or molecular groups has attracted much attention. It offers a possible way to modify the electronic, chemical, optical, and mechanic properties of SWCNTs.[1–3] Experimentally, functionalization of SWCNTs can be realized by introducing molecules or molecular groups to their open ends or on their walls,[2,3] through carbodiimide chemistry,[4] or mixing the SWCNTs with an electrophilic reagent.[2,3] Molecules such as NH_3, NO_2, and O_2 can dramatically change the electronic and transport properties of SWCNTs,[5–8] which could lead to giant thermopower effects.[9] Theoretically, computational studies based on density functional theory (DFT) have been carried out to investigate the mechanism behind the functionalization of SWCNTs by molecules or molecular groups.[9–16] It was found that the adsorbed molecules or atoms changed the sp^2 local hybridization and lead to the formation of π-π conjugated bonds at the surface of the SWCNT.

Recently, effects of OH groups on the electronic properties of SWCNTs were systematically investigated. It was found that electronic properties of SWCNTs can be greatly changed due to the introduction of the OH group. Furthermore, contrary to the effect of oxygen as reported in Ref. 16, the OH group does not etch the tube as a result of oxidization. The OH doping can be an effective mechanism for modifying the electronic properties of SWCNTs, which makes SWCNTs a possible candidate for biological sensors. It can be expected that OH attached SWCNT bundles exhibit thermopower effect due to the additional scattering channel for electrons in the tube wall.

To further understand the effect of OH doping on SWCNTs, we carried out *ab initio* total energy calculations[17] on the electrical and optical properties of single wall carbon nanotubes attached with OH groups. A semiconducting SWCNT was chosen in our calculations since the effects of OH groups would be more apparent for a semiconducting SWCNT than its metallic counterpart.

The first-principles method based on the density functional theory[18] and the generalized gradient approximation[19] (GGA) are used in our study to investigate the structural and electronic properties of SWCNTs attached with OH groups. In our calculation, we used the plane-wave basis DFT pseudopotential method[18] and the CASTEP code.[17] The ionic potentials are described by the ultrasoft nonlocal pseudopotential proposed by Vanderblit.[20] The Monkhorst and Pack scheme of *k*-point sampling was used for integration over the first Brillouin zone.[21] The Kohn-Sham energy functional is directly minimized using the conjugate-gradient method.[22] An energy cutoff of 400 eV and six *k* points along the axis of the tube in the reciprocal space were used in our calculation. Good convergence was obtained with these parameters and the total energy was converged to 2.0×10^{-5} eV/at. A large supercell dimension in the plane perpendicular to the tube axis was used to avoid interaction between the carbon nanotube and its images in neighboring cells. The unit is periodic in the direction of the tube with a cell height of 4.24 Å (see Fig. 1).

Calculations were carried out for a zigzag (10×0) SWCNT, with and without the OH group, respectively. One OH group was included in each unit cell to simulate the adsorption and it was chemically attached to the wall of the nanotube. The geometry of the SWCNT, with and without the OH group, was fully optimized. Figure 1 shows the optimized structure of the OH functionalized SWCNT (10×0) with the oxygen atom attached to the wall. Properties of the carbon nanotubes such as band structure, density of states (DOS), and population analysis were calculated for the optimized structure.

The binding energy of the OH group was calculated according to the following:

$$E_b = E_t(CNT + OH) - E_t(CNT) - E_t(OH), \qquad (1)$$

where $E_t(CNT+OH)$ and $E_t(CNT)$ are the total energies of the tube, with and without the OH group, respectively,

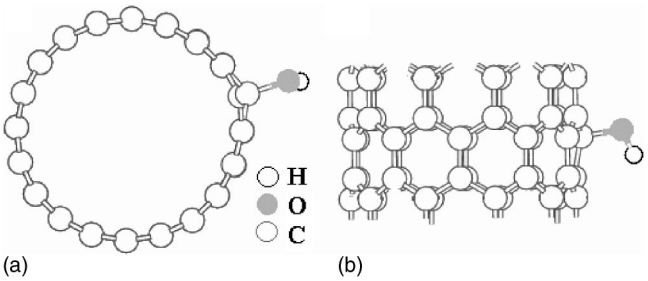

FIG. 1. (a) Top and (b) side views of the SWCNT-OH supercell used in our calculation. One OH group is attached on the wall of the SWCNT with the oxygen atom onnected to the carbon atom.

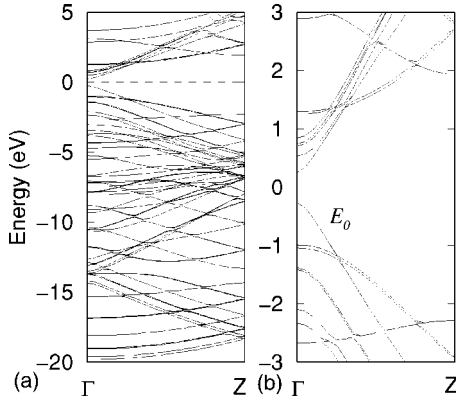

FIG. 2. (a) Band structure of the zigzag (10×0) SWCNT. (b) shows its details near the Fermi level (E_F=0 eV).

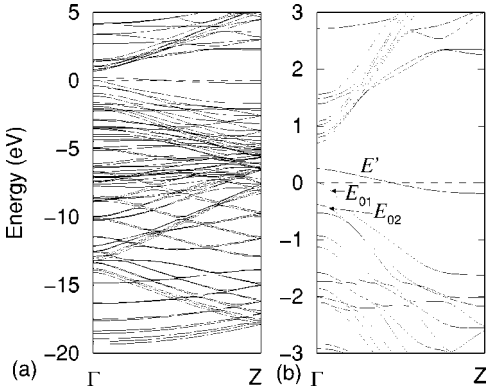

FIG. 3. (a) Band structure of the SWCNT-OH system. (b)shows its details near the Fermi level (E_F=0 eV).

$E_t(OH)$ is the total energy of an isolated OH group. The binding energy was found to be 0.78 eV.

The band structure of the zigzag (10×0) carbon nanotube, which has the D_{10h} symmetry, is shown in Fig. 2. Most of the energy levels are doubly degenerate, which is a general property for the achiral carbon nanotubes due to the rotational point group C_n. Our calculated result is very similar to that in Ref 23. Figure 2(b) shows the fine structure of the bands near the Fermi level. It can be seen that there exists a band gap that is about 0.51 eV within GGA. The highest valence band consists of two degenerate levels, denoted as E_0 in Fig. 2(b), which contributes to the big π bond along the ring of the tube.[24] The bottom of the conduction band corresponds to the big π^* antibonding states.

In the optimized tube-OH system, the angle between the C-O bond and the O-H bond is about 100°. It is well known that the three *p* orbitals of oxygen are perpendicular to each other. The bond of the *sp* hybridization formed by one *p* orbital (p_z) of oxygen and the *s* orbital of hydrogen is roughly perpendicular to the C-O bond because another *p* orbital (p_x) of oxygen forms a bond with one *p* orbital of the carbon. The angle is tilted due to the interaction of orbitals. By carefully analyzing the bonding around the carbon atom on which the OH group is attached, we found that the angles between the O-C bond and C-C bond fall in the range of 107°–112°, and are close to 109.5° of sp^3 hybridization. And the bond lengths are within 1.48 and 1.52/Å. It can be concluded that the local sp^2 hybridization was destroyed due to the introduction of the OH group, and a $pp\sigma$ bond was formed between C and O. The local structure of the carbon nanotube is distorted due to the introduction of the OH group, and C-C bond becomes longer than that in a pure SWCNT (1.42 Å). This distortion and the addition of the OH group lead to the differences in the electronic properties of the SWCNT-OH system and pure SWCNT.

The band structure of the carbon nanotube is changed significantly upon introduction of the OH group, as can be seen in Fig. 3. It is clear that an energy level, E' crosses the Fermi level (E_F=0). The fine band structure near E_F [Fig. 3(b)] shows that the degenerate energy levels below the Fermi level split after the OH group is introduced to the tube (refer to Fig. 2). The original doubly degenerate state (E_0) in the pure tube splits into two states E_{01} and E_{02} which are separated by 0.39 eV at the Γ point in the SWCNT-OH system. This energy level separation is due to the reduced symmetry of the system after the OH group is introduced.

The E_0 state consists of the big π bonding in the pure tube. Figure 4(a) shows the electron density of this orbital. The π bonding characteristics is clearly seen in the figure. Analysis of electron density of the corresponding orbitals in the tube-OH system reveals the mechanism behind the separation of the doubly degenerate E_0 state. The E_0 state of the perfect tube [Fig. 4(a)] interacts with the one *p* orbital (p_y) of the oxygen, and results in the separation of E_0 into E_{01} and E_{02}, as shown in Fig. 3(b). The electron densities of these orbitals show that E_{02} and E' are the coupling state and anticoupling state between the E_0 and p_y orbital of oxygen, respectively, shown in Figs. 4(d) and 4(b) respectively, while E_{01} is mainly contributed by the big π bond of the tube [Fig. 4(c)]. This is different from the attachment of oxygen molecule.[11]

The calculated total density of states (TDOS) further revealed the separation of the degenerate states and the expan-

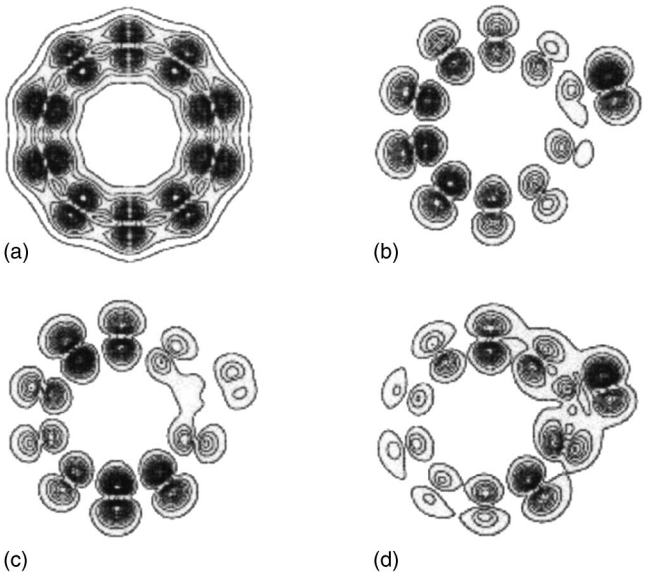

FIG. 4. Electron density corresponding to (a) the E_0 level in the pure tube, (b) the E' level crossing the Fermi level, (c) the E_{01} level and, (d) the E_{02} level in the tube-OH system, respectively.

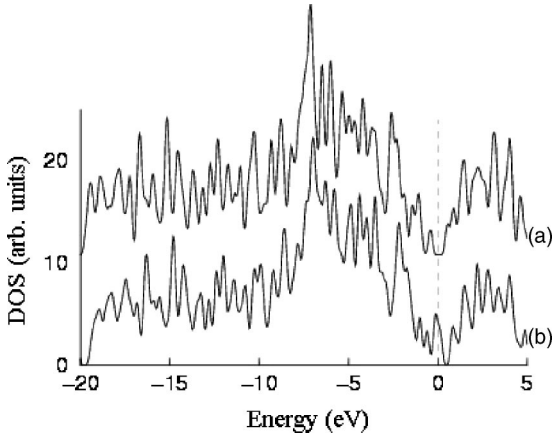

FIG. 5. Calculated (a) total DOS of the pure SWCNT, and (b) total DOS of SWCNT-OH. The Fermi level is at 0 eV.

sion of the DOS. Figure 5 shows the TDOS of the pure tube (a) and the TDOS of the tube-OH system (b), respectively. Notable differences can be seen in the densities of states, which are a result of introducing the OH group to the nanotube. When the OH group is introduced to the tube wall, a peak in the DOS arises at the Fermi level and the energy gap is significantly reduced. This is due to the interaction between the tube and the oxygen because the p_x orbital of oxygen and the p orbital of one carbon atom form a bond, which makes the degenerate levels in the pure SWCNT to split. The OH group possesses an unpaired electron, which actively participates in hybridization near the C atom when it is attached to the tube. This can form an acceptor level and enhance the conductivity of the CNT. Changes in the TDOS can also be seen in other ranges of energy but are minor. The main features in the TDOS of the pure tube remain in the TDOS of the tube-OH system, due to the fact that the TDOS in these regions are dominated by the carbon states.

When the OH group is attached to the tube wall, electrons are transferred from the tube to the OH group due to its large electronic negativity. From the Mulliken population analysis, we found a charge transfer of 0.33e per O atom. We can therefore conclude that semiconducting SWCNTs can be functionalized and their band gaps can be significant reduced by the attachment of organic molecules. Also, it can be expected that SWCNTs maintain their electronic properties due to hole carriers generated in the tube. The calculated length of the C-O bond is 1.52 Å, which is similar to the bond length of C-O in aromatic carbon.[25] This property shows that the functionalized SWCNTs can have good solubility and will be useful in biology and chemistry. In our calculation, there is only one OH group in each unit cell. If there was one OH group per six carbons, as in the aromatic carbon, the tube can be expected to be an aromatic tube. Further experiments and calculations will be carried out to explore its property.

Theoretical studies of the optical and loss spectra of SWCNTs and multiwalled carbon nanotubes (MWCNTs) have been reported previously,[26–29] which illustrated that the optical properties of CNTs show a special structure at $\omega \sim 2\gamma_0$ ($\gamma_0 \sim 2.3$–3.0 eV is the nearest-neighbor overlap integral[30]) for MWCNTs.[28] In this work, we calculated the loss function which is a direct probe of the collective excitation of the system under consideration. We compare the loss functions of the two models to investigate the effect of OH doping on plasma frequency. The imaginary part of the dielectric constant was calculated from

$$\varepsilon_2(q \to O_w, \hbar\omega) = \frac{2e^2\pi}{\Omega\varepsilon_0} \sum_{k,v,c} |<\Psi_k^c|\hat{u}\cdot r|\Psi_k^v>|^2 \times \delta(E_k^c - E_k^v - E), \quad (2)$$

where $\hat{u}$ is the vector defining the polarization of the incident electric field. This expression is similar to the Fermi's Golden rule for time-dependent perturbations, and $\varepsilon_2(\omega)$ can be thought of as detailing the real transitions between occupied and unoccupied electronic states. The real part, $\varepsilon_1(\omega)$, is obtained by the Kramers-Kronig relation. The loss function is calculated using $\mathrm{Im}[-1/\varepsilon(\omega)]$ at zero momentum transfer from the macroscopic dielectric function $\varepsilon(\omega)[\varepsilon(\omega)=\varepsilon_1(\omega) + i\varepsilon_2(\omega)]$ for a periodic system.

Figure 6(a) shows the loss function of the zigzag (10 $\times$0) SWCNT. Several peaks are observed, which are related to the one-dimensional (1D) subbands with divergent density of states. One pronounced peak in the loss function is at $\omega \sim 2\gamma_0$, which can be attributed to the collective excitations of π electrons.[28] The π plasmon is weaker for the perpendicular polarization than for the parallel polarization, since the optical excitation is less effective in the perpendicular case. Another pronounced peak is at $\omega \sim 17.0$–19.0 eV. The peaks are attributed to the higher-frequency $\pi+\sigma$ plasmon.[27] Under the perpendicular polarization, there is a peak around $\omega \sim 2.6$ eV. The lower-frequency excitation only exists in the SWCNTs, which is related to the inter-π-band excitation.[31] Figure 6(b) shows the loss function of the SWCNT-OH system. Significant differences can be observed when it is compared with Fig. 6(a). The π plasmon excitation disappears in the SWCNT-OH system. The inter-band excitation becomes stronger in both polarization conditions at the lower frequency ($\omega \sim 1.8$–2.7 eV). It is also noticed that the higher-frequency excitation is downshifted to 16–18 eV with reduced strength. The reason behind thes e changes is the introduction of the OH group. As we analyzed above, the introduction of the OH distorted the symmetry of the tube and split the degenerate energy levels. The separation increases the number of energy levels and reduces the spacing of energy levels, which leads to more inter-band excitation and the downshift of excitation energy. At the same time, the big π bonding was distorted due to the introduction of the OH that forms bond with the tube. The distortion disturbed the π electron gas and made the π plasmon to disappear. The downshift and reduction of the higher-frequency $\pi+\sigma$ plasmon can be attributed to the same reason.

In summary, the attachment of the OH group on the tube wall gives rise to significant changes in the electronic properties of the semiconducting SWCNT. It has been found that the charge transfer from the carbon to the oxygen is an important mechanism in the change of the conductivity in the SWCNT-OH system. From the calculated band structure, an acceptor level in the SWCNT-OH system was found, which mainly comes from anticoupling state between the p_y orbital

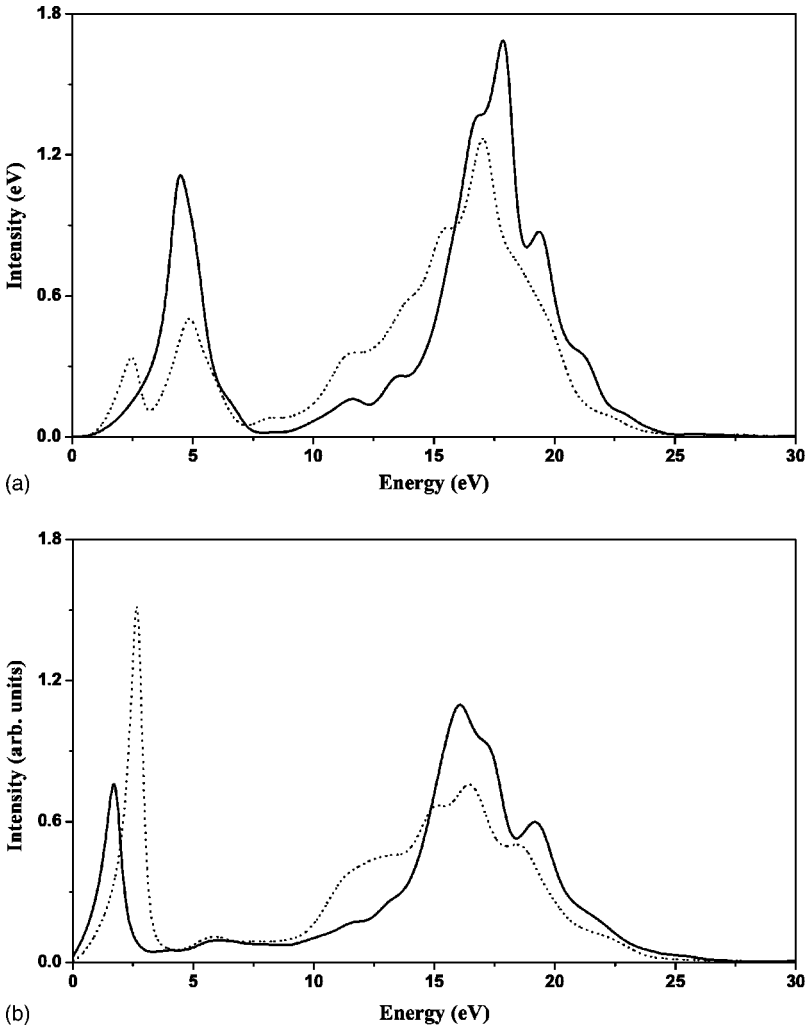

FIG. 6. Loss functions (a) of zigzag (10×0) SWCNT and (b) the SWCNT-OH system. The dotted line (solid line) corresponds to the case when the polarization direction is perpendicular (parallel) to the axis of the tube, respectively.

of the oxygen and big π state of the tube. This strongly suggests that the OH group accepts electrons from the tube, which is in agreement with the Mulliken population analysis. The interaction between the tube and oxygen makes the degenerate levels in the pure tube to split. Based on the results of our calculations, the OH group is expected to be a good acceptor for hole doping. Introducing the OH group can be an effective way of modifying the electronic properties of semiconducting SWCNTs. The OH-doped SWCNTs can be a useful biological sensor. It is also found that introducing the OH group makes the π plasmon excitation disappear and enhances the inter-π-band excitation. Our results also suggest that optical measurement can be used to distinguish tubes with and without OH attachment.

*Corresponding author: Email address phyfyp@nus.edu.sg

[1] C. Richard, F. Balavoine, P. Schultz, T. W. Ebbesen, and C. Mioskowski, Science **300**, 775 (2003).
[2] J. Chen, M. A. Hamon, H. Hu, Y. Chen, Apparao M. Rao, P. C. Eklund, and R. C. Haddon, Science **282**, 95 (1998).
[3] S. S. Wong, E. Joselevich, A. T. Woolley, C. L. Cheung, and C. M. Lieber, Nature (London) **394**, 52 (1998).
[4] J. Liu, A. G. Rinzler, H. Dai, J. H. Hafner, R. K. Bradley, P. J. Boul, A. Lu, T. Iverson, K. Shelimov, C. B. Huffman, F. Rodriguez-Macias, Y. Shon, T. R. Lee, D. T. Colbert, and R. E. Smalley, Science **280**, 1253 (1998).
[5] S. Peng and K. Cho, Nanotechnology **11**, 57 (2000).
[6] J. Kong, N. R. Franklin, C. Zhou, M. G. Chapline, S. Peng, K. Cho, and H. Dai, Science **287**, 622 (2000).
[7] J. Zhao, A. Buldum, J. Han, and J. Lu, Nanotechnology **13**, 195 (2002).
[8] X. P. Tang, A. Kleinhammes, H. Shimoda, L. Fleming, K. Y. Bennoune, S. Sinha, C. Bower, O. Zhou, and Y. Wu, Science **288**, 492 (2000).
[9] J. Zhao, J. Lu, J. Han, and C. Yang, Appl. Phys. Lett. **82**, 3746 (2003).
[10] H. Chang, J. Lee, S. M. Lee, and Y. H. Lee, Appl. Phys. Lett. **79**, 3863 (2001).
[11] S. H. Jhi, S. G. Louie, and M. L. Cohen, Phys. Rev. Lett. **85**, 1710 (2000).
[12] E. C. Lee, Y. S. Kim, Y. G. Jin, and K. J. Chang, Phys. Rev. B **66**, 073415 (2002).
[13] D. J. Mann and M. D. Halls, J. Chem. Phys. **116**, 9014 (2002).

[14] P. Giannozzi, R. Car, and G. Scoles, J. Chem. Phys. **118**, 1003 (2003)
[15] A. N. Andriotis, M. Menon, D. Srivastava, and G. Froudakis, Phys. Rev. B **64**, 193401 (2001)
[16] C. Y. Moon, Y. S. Kim, E. C. Lee, Y. G. Jin, and K. J. Chang, Phys. Rev. B **65**, 155401 (2002)
[17] M. D. Segall, P. J.D. Lindan, M. J. Probert, C. J. Pickard, P. J. Hasnip, S. J. Clark, and M. C. Payne, J. Phys.: Condens. Matter **14**, 2717 (2002).
[18] M. C. Payne, M. P. Teter, D. C. Allan, T. A. Arias, and J. D. Joannopoulos, Rev. Mod. Phys. **64**, 1045 (1992).
[19] J. P. Perdew and Y. Wang, Phys. Rev. B **46**, 13 244 (1992).
[20] D. Vanderblit, Phys. Rev. B **41**, 7892 (1990).
[21] H. J. Monkhorst and J. Pack, Phys. Rev. B **13**, 5188 (1976).
[22] M. P. Teter, M. C. Payne, D. C. Allan, Phys. Rev. B **40**, 12 255 (1989).
[23] M. S. Dresselhaus, G. Dresslhaus, and P. C. Eklund, *Science of Fullerenes and Carbon Nanotubes* (Academic Press, San Diego, 1996).
[24] S. Reich and C. Thomsen, and P. Ordejon, Phys. Rev. B **65**, 155411 (2002).
[25] A. A. Askadskii, *Computational Materials Science of Polymers* (Cambridge International Science, Cambridge, 2003).
[26] F. J. Garcý'a-Vidal, J. M. Pitarke, and J. B. Pendry, and Phys. Rev. Lett. **78**, 4289 (1997).
[27] A. G. Marinopoulos, L. Reining, A. Rubio, and N. Vast, Phys. Rev. Lett. **91**, 046402 (2003).
[28] M. F. Lin, F. L. Shyu, and R. B. Chen, Phys. Rev. B **61**, 14 114 (2000).
[29] M. F. Lin, Phys. Rev. B **62**, 13 153 (2000).
[30] J. W. Mintwire, B. I. Dunlap, and C. T. White, Phys. Rev. Lett. **68**, 631 (1992).
[31] T. Pichler, M. Knupfer, M. S. Golden, J. Fink, A. Rinzler, and R. E. Smalley, Phys. Rev. Lett. **80**, 4729 (1998).